Solvent/Solute Interactions Probed by Picosecond Transient Raman Spectroscopy: Mode Specific Vibrational Dynamics of S1 trans-Stilbene

ARTICLE *in* THE JOURNAL OF PHYSICAL CHEMISTRY · OCTOBER 1992

Impact Factor: 2.78 · DOI: 10.1021/j100201a047

4 AUTHORS, INCLUDING:

William L. Weaver
La Salle University
133 PUBLICATIONS **189** CITATIONS
SEE PROFILE

Koichi Iwata
Gakushuin University
77 PUBLICATIONS **1,142** CITATIONS
SEE PROFILE

Terry Gustafson
The Ohio State University
129 PUBLICATIONS **2,203** CITATIONS
SEE PROFILE

Solvent/Solute Interactions Probed by Picosecond Transient Raman Spectroscopy: Mode-Specific Vibrational Dynamics in S_1 *trans*-Stilbene

William L. Weaver, Lisa A. Huston, Koichi Iwata,† and Terry L. Gustafson*

Department of Chemistry, The Ohio State University, 120 West 18th Avenue, Columbus, Ohio 43210-1173
(Received: June 1, 1992; In Final Form: July 15, 1992)

We obtain the picosecond transient Raman spectra of S_1 *trans*-stilbene in acetonitrile and *n*-hexane. We observe mode-specific, solvent-dependent variations in the vibrational spectra. In acetonitrile, the vibrational bands in S_1 *trans*-stilbene associated with the phenyl portion of the molecule shift to higher energy and increase in bandwidth, relative to *n*-hexane, owing to the increased coupling of the excited state to the more polar solvent. In both solvents, the vibrational motions associated with the olefin portion of the molecule change peak position and bandwidth with delay, while the peak position and bandwidth of the phenyl modes in each solvent remain constant with delay. The change in peak position and bandwidth of the olefin modes depends on the excitation frequency used to excite the molecule. We attribute these changes, in part, to vibrational relaxation via resonance energy exchange involving low-frequency vibrations. Additional factors, likely attributable to conformational changes, appear to give rise to a portion of the effects we observe.

1. Introduction

While much is understood on a macroscopic scale about the interactions that occur between solute and solvent in solution, the microscopic details, involving the interaction potentials between solvent and solute, transport processes, and energy transfer, are not well-understood. The last decade has seen considerable effort, both experimental and theoretical, aimed at elucidating the role of solvent dynamics in chemical reaction rates. Much of this work has been reviewed.[1-6] A typical experiment involves photoexcitation of a probe molecule in a given solvent or solvent series and monitoring the reaction rate spectroscopically, often as a function of temperature or pressure. The reaction can be as simple as the rotation of a molecule in solution or as complex as electron-transfer processes in biological systems. The primary spectroscopic methods have been based on electronic spectroscopies (i.e., absorption and fluorescence). The rates of the reaction are then compared to bulk solvent properties, since the solvent is viewed from the perspective of statistical mechanics as "noninteracting". That is, the solvent molecules simply act as a heat bath and may be considered as a continuous viscous medium at liquid-phase densities. Recent studies suggest that the concept of a noninteracting solvent is not completely rigorous, depending on the specific molecular system and the solvent involved.[7-11]

Photoisomerization reactions, particularly the photoisomerization of *trans*-stilbene (tS), have been widely used to probe solvent/solute interactions.[7,8,11-17] The photochemistry of tS has been studied extensively.[18] The well-known photoisomerization reaction coordinate, as first proposed by Saltiel,[19] involves the activated twisting of the central double bond on the lowest excited-state singlet surface (i.e., $^1t^* \rightarrow {}^1p^*$). Following Hochstrasser's initial application,[18c] the rates for the twisting about the central double bond have been modeled using Kramers' theory,[20] where the motion of the molecule over the barrier is described in terms of Brownian motion on a one-dimensional potential surface. In order to obtain good agreement between the experimental rates and Kramers' theory, it has been necessary to include various modifications. A fundamental assumption in most of the theories is that the friction coefficient is proportional to the shear viscosity of the solvent, as predicted by the Stokes-Einstein hydrodynamic equation.[21] Based on this assumption, several groups have proposed a frequency-dependent friction coefficient in order to reconcile experiment and theory.[5,22-26] While the model provides a good fit between the experimental results and theory, the parameters that are extracted for the barrier give unrealistic frequencies. Others have proposed that the actual reaction coordinate is not one-dimensional but multidimensional, while still adhering to the hydrodynamic model for solvent friction.[27-31] Recently, Saltiel and co-workers have suggested that the disagreement between theory and experiment can be explained by the failure of the Stokes-Einstein approximations in describing the microviscosity of the solvent.[14,15] Using the translational diffusion coefficient of the rotating portion of the excited stilbene molecule, they propose a medium enhanced barrier model that provides excellent agreement to Kramers' one-dimensional theory.[14]

While the rates of the reactions have provided significant insight into solvent/solute interactions, it is clear that direct structural information about the specific interactions between a solute and its solvent environment would be of interest. Recently, MacPhail and co-workers have used ground-state Raman spectroscopy to study the solvent friction dependence of torsional, rotational, and conformational dynamics in small molecules.[32] Other workers have shown that resonance Raman spectroscopy[33] and ultrafast vibrational spectroscopy of transient species[34-38] provide information about the flow of energy between solute and solvent. In general, the transient vibrational spectroscopies have only been able to observe effects, such as vibrational cooling, that affect the entire spectrum; no mode-specific effects have been observed.

We are using the photoisomerization of tS, as probed with picosecond transient Raman spectroscopy, to study solvent/solute interactions. There are several reasons for choosing to use tS as the probe molecule. First, the dynamics are well-understood in many different solvents. Therefore, we have a priori control over the time range and effective "friction" associated with the solvent interaction. Second, the spectroscopic properties of the system are very favorable for high signal-to-noise transient Raman experiments.[39-46] The transient absorption is very strong, and the wavelengths for pump and probe are in readily available spectral regions. Third, many substituted analogues of tS are readily available. The analogues provide us with the ability to change selectively the chemical or physical properties involved in solvation. And fourth, the vibrational spectra of both the ground and excited states are well-understood. A complete analysis has been done for the vibrational spectrum of S_0 tS by several groups.[47-50] The individual studies vary slightly, but the general agreement is quite good. In addition, a normal coordinate analysis has been done on S_1 tS.[51,52] While more work remains to be done, the results for S_1 are consistent with existing data, including the results for the S_1 spectra of a number of deuterated and ^{13}C-labeled stilbenes.[39,43,44,53]

Hamaguchi[40] and Kamalov et al.[42] have seen evidence for "hot" S_1 tS in the transient Raman spectrum using optical depletion timing. However, no "real time" dynamics have been obtained to establish the nature of the processes that give rise to the observed changes. In this work, we show that the interactions that occur between the solvent and tS on the S_1 potential surface result in

* Author to whom correspondence should be addressed.
† Present address: Molecular Spectroscopy Laboratory, Kanagawa Academy of Science and Technology, KSP East 301, 3-2-1 Sakato, Kawasaki 213, Japan.

0022-3654/92/2096-8956$03.00/0

TABLE I: Observed and Calculated Raman Shifts (in cm^{-1}) of S_1 *trans*-Stilbene in *n*-Hexane and Acetonitrile with the Approximate Vibrational Assignments

obsd shift at 10 ps in			
n-hexane	acetonitrile	calcd shift[a]	approx potential energy distribution[a]
1564	1567	1572	C_o=C_o str 55, C_o—Ph str 34, C_o—H bend 15
1528	1544	1529	C=C str 73, C—H bend 41, CCC def 11
1464	1465	1466	C—H bend 67, C—C str 29
1420	1421	1407	C—H bend 68, C—C str 35
1254	1256	1263	C_o—H bend 59, C—C str 16
1239	1243	1236	C—C str 95, C—H bend 16
1178	1179	1176	C—H bend 22, C_o=C_o str 19, C_o—Ph str 19
1146	1150	1160	C—H bend 43, C—C str 34

[a] From ref 51.

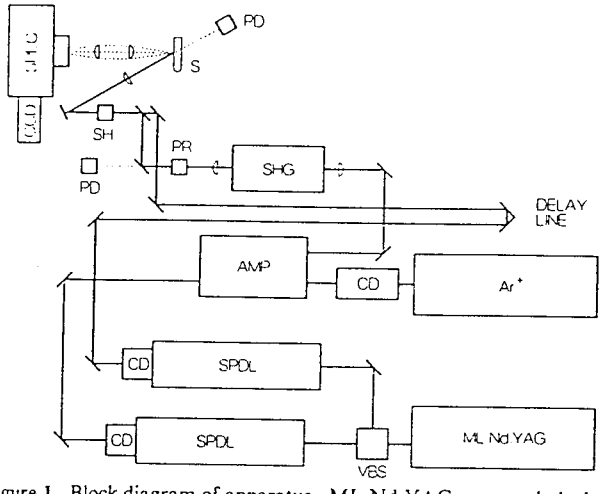

Figure 1. Block diagram of apparatus. ML Nd:YAG: cw, mode-locked Nd^{3+}:YAG laser. VBS: variable-beam splitter. SPDL: synchronously pumped dye laser. CD: cavity dumper. AMP: six-pass dye laser amplifier. Ar^+: argon ion laser. SHG: second harmonic generator. PR: polarization rotator. PD: photodiode. SH: shutter. S: sample. SPEC: spectrograph. CCD: charge-coupled-device optical multichannel analyzer.

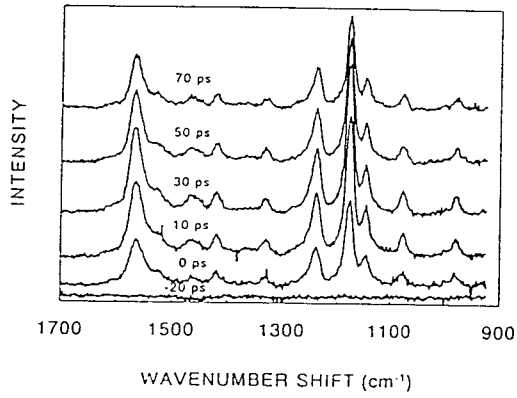

Figure 2. S_1 transient Raman spectra of *trans*-stilbene in *n*-hexane at various delays from −20 to 70 ps after photoinitiation at 294.4 nm from the region of 900 to 1700 cm^{-1}: probe, 577 nm; repetition rate, 1 MHz. Each delay represents the unsmoothed spectrum obtained by 20 min of total observation time.

mode-specific, solvent-dependent variations in the picosecond transient Raman spectrum. We observe shifts in the peak positions and changes in the bandwidths of several vibrational bands, depending on the solvent and delay. In order to investigate the role of vibrational relaxation in this process, we have obtained the time dependence of the transient Raman spectra of tS at different excitation wavelengths, keeping the probe wavelength fixed. This provides a controlled way of introducing excess vibrational energy into the system. We compare our results to the various theories of how tS is thought to interact microscopically with its solvent environment.

2. Experimental Section

We have previously described the MHz laser system that we use to obtain the picosecond transient Raman spectra.[43,44,46] We have recently made several modifications to the apparatus. Figure 1 shows a block diagram of the existing apparatus. Briefly, the second harmonic of a continuous wave (cw) mode-locked Nd:YAG laser (Coherent, Inc., Model Antares 76S) is used to pump two independently tunable synchronously pumped, cavity-dumped dye lasers (Coherent, Inc., Models 702-2 and 702-3), each with R6G (Exciton Corp.) as the excitation medium and DQOCI (Exciton Corp.) as the saturable absorber. The output from one of the dye lasers is amplified at Megahertz repetition rates with a six-pass amplifier pumped by 1.7 W at 514.5 nm from a cavity-dumped argon ion laser (Coherent, Inc., Model Innova 200).[54] The extraction efficiency of the amplifier is 15–20%, providing >200-nJ, 3-ps pulses at 1 MHz. The amplified output is frequency-doubled using a temperature-tuned ADA crystal (Inrad Model 5-15) to generate ~20-nJ, 3-ps pulses in the region of ca. 280–310 nm. The visible probe pulse (ca. 577-nm, 30-nJ, 3-ps pulses) traverses an optical delay line (Compumotor F-L5A-P54) before being combined colinearly with the UV pump pulse and focused on the sample with a 5-cm lens. The polarization of the pump and probe beams can be independently controlled; for this work, the polarization is set to the magic angle (54.7°) to remove contributions from rotational reorientation to the observed transient Raman signals.[55] The pump and probe impinge on a spinning sample cell at ~45°, and the backscattered Raman signal is dispersed through a single spectrograph (ISA THR640) using a 600 groove/mm grating. A CCD optical multichannel analyzer (Photometrics CC200 System with Thomson-CSF 576 × 384 chip) is used to detect the signal. We monitor the pump and probe intensities using reflections of the beams, integrating with photodiodes (United Detector Technology) to normalize individual spectra for fluctuations in the laser power. The shutter for the CCD is placed before the sample, thereby preventing photodegradation of the sample by illuminating the sample only during spectral acquisition. The ultimate time resolution of the system is limited by the timing jitter between the dye lasers and is measured to be ~8 ps. Data acquisition is controlled by an IBM AT compatible computer running software written in ASYST (Asyst Software Technologies). The wavenumber shift is calibrated using the Raman spectra of benzene, CCl_4, and acetone. Data collection times were 20 min at each delay. The *trans*-stilbene was purchased from Kodak (scintillation grade) and was used without further purification. The solvents used in this study were *n*-hexane (Aldrich, 99+%) and acetonitrile (Aldrich, 99.5+%). The spectral features were fit on an IBM AT compatible computer using software written in ASYST.

3. Results

We have obtained transient Raman spectra of tS in *n*-hexane and acetonitrile over the range from 170 to 1700 cm^{-1} at various delays. For tS in *n*-hexane, we have used three different excitation wavelengths, 303.2, 294.4, and 285.7 nm, corresponding to ~1800, ~2800 and ~3800 cm^{-1} of excess vibrational energy, respectively, above the origin for tS (ca. 31 200 cm^{-1}). In Figures 2 and 3, we show the spectra of S_1 tS in *n*-hexane and acetonitrile, respectively, over the range from 900 to 1700 cm^{-1} at delays of −20, 0, 10, 30,

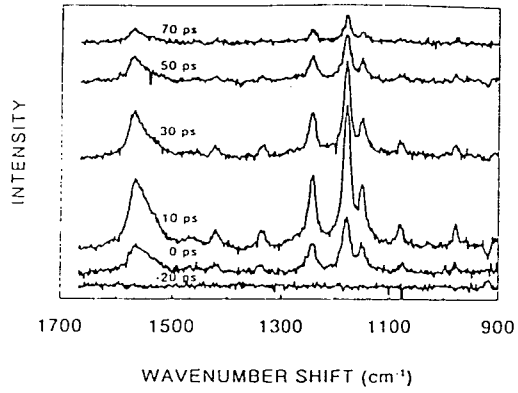

Figure 3. S_1 transient Raman spectra of *trans*-stilbene in acetonitrile at various delays from −20 to 70 ps after photoinitiation at 294.4 nm from the region of 900 to 1700 cm^{-1}: probe, 577 nm; repetition rate, 1 MHz. Each delay represents the unsmoothed spectrum obtained by 20 min of total observation time.

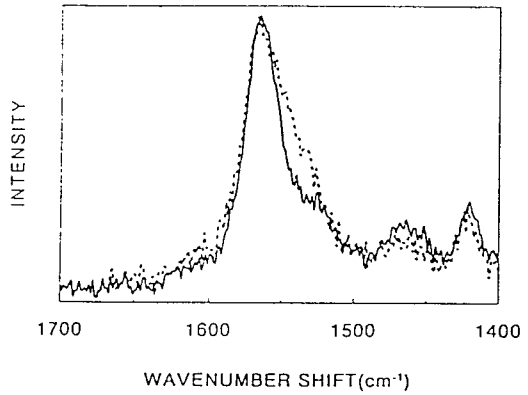

Figure 4. Ten-picosecond delay spectrum of S_1 *trans*-stilbene in acetonitrile (dashed line) normalized to the 10-ps delay spectrum of S_1 *trans*-stilbene in *n*-hexane (solid line) over the region 1400–1700 cm^{-1}: pump, 294.4 nm; probe, 577 nm; repetition rate, 1 MHz for both spectra.

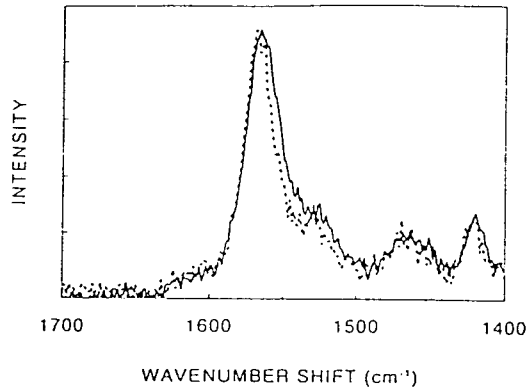

Figure 5. Seventy-picosecond delay spectrum of S_1 *trans*-stilbene in *n*-hexane (dashed line) normalized to the 10-ps delay spectrum of S_1 *trans*-stilbene in *n*-hexane (solid line) over the region 1400–1700 cm^{-1}: pump, 294.4 nm; probe, 577 nm; repetition rate, 1 MHz for both spectra.

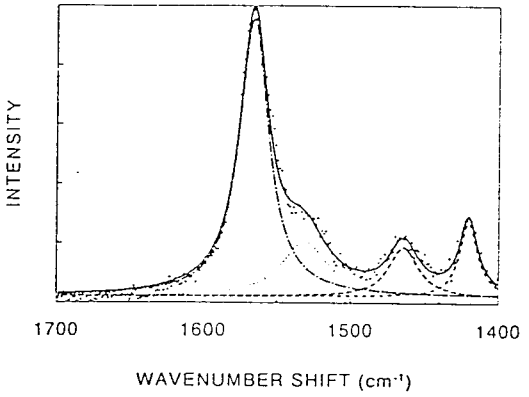

Figure 6. Typical fit to Lorentzian line shapes for the S_1 transient Raman spectrum of *trans*-stilbene in *n*-hexane: pump, 294.4 nm; probe, 577 nm; repetition rate, 1 MHz.

50, and 70 ps. The excitation wavelength for these data is 294.4 nm; the probe wavelength is 577 nm. In Table I, we summarize the band positions in each solvent and the approximate assignments of the S_1 vibrational bands over the range from 1100 to 1700 cm^{-1}. The assignments are based on the normal mode calculation of Tasumi and co-workers.[51] In Figure 4, we compare the spectra of S_1 tS in *n*-hexane and acetonitrile over the range from 1400 to 1700 cm^{-1} obtained at the same pump and probe wavelengths at a delay of 10 ps. In order to show more clearly the types of changes that occur in the transient spectra for a given solvent, in Figure 5 we compare the normalized S_1 spectra of tS in *n*-hexane at delays of 10 and 70 ps over the range from 1400 to 1700 cm^{-1}. The excitation wavelength for these data is 294.4 nm. For each spectrum, we have fit the observed vibrational bands to Lorentzian line shapes and obtained peak positions, bandwidths, and integrated intensities. We note that the peaks do not fit well to Gaussian line shapes. In Figure 6, we show a typical fit to the data in the region from 1400 to 1700 cm^{-1} obtained for S_1 tS in *n*-hexane at a delay of 20 ps. We emphasize that the quality of the spectra is such that we can obtain good fits to the data at all delays.

4. Discussion

As can be seen from the data, we observe two types of variations in the Raman spectra of S_1 tS. The first is the change in the nominal peak positions of the various bands in different solvents. The second is the change in the peak position and bandwidth of certain bands as the delay is changed. In order to interpret our results, we will first discuss the assignments of the bands. Second, we will discuss the variations in the nominal peak positions and bandwidths with different solvents. Then, we will consider the variations in the peak positions and bandwidths with changes in the delay.

Our understanding of these data is based on the proper assignment of the vibrational bands in the excited state. We will concentrate our discussion on the vibrational bands in the C=C stretch region, from 1500 to 1700 cm^{-1}, although similar effects are observed for vibrational bands in other regions of the spectrum, specifically the bands at ~1180 and ~1240 cm^{-1}. The ground-state spectrum of tS contains two bands in the C=C stretch region, at 1639 and 1598 cm^{-1}. The higher frequency band corresponds to the olefinic C=C stretch, and the lower frequency band corresponds to the phenyl C=C stretch. For the corresponding peaks in the excited state, we observe two broad, overlapping bands at ~1565 and ~1528 cm^{-1}. The exact frequency of these two bands is dependent upon the solvent and the delay. The two peaks at ca. 1565 and 1528 cm^{-1} correspond to motions involving predominately the C=C stretch of the olefin and phenyl portions of the molecule, respectively. (See Table I.) It is important to emphasize that there is substantial mixing of the vibrational modes in S_1 tS.[52] Therefore, the olefinic C=C stretch in S_1 tS is not as "pure" as it is in S_0 tS.

Given the approximate band assignments, we can now compare the peak positions and bandwidths of S_1 tS in *n*-hexane and acetonitrile. As can be seen from the data presented in Table I, most of the peak positions remain fairly constant between the two solvents at early delay times. The only band that exhibits a substantial peak shift is the phenyl C=C stretch at 1528 cm^{-1} in *n*-hexane and 1544 cm^{-1} in acetonitrile. In addition to the shift in the peak position to higher frequency in acetonitrile, the bandwidth of the phenyl C=C stretch increases from 33 to 43 cm^{-1}. We note that the bandwidth of the olefin C=C stretch at a delay of 10 ps is 24 cm^{-1} in both *n*-hexane and acetonitrile. The changes in the phenyl mode are readily observable in the data plotted in Figure 4. The viscosities of *n*-hexane and acetonitrile are similar, 0.294 and 0.345, respectively. However, the dielectric constants for the two solvents are quite different: 1.88 for *n*-

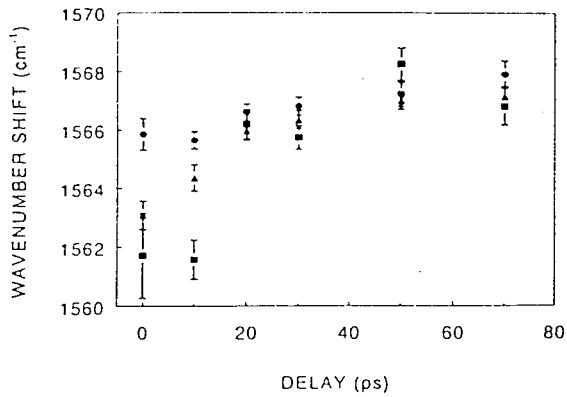

Figure 7. Peak position of the olefin C=C stretching vibration of S_1 *trans*-stilbene in *n*-hexane vs delay for three pump wavelengths: 303.2 nm (●); 294.4 nm (▲); 285.7 (■); probe, 577 nm; repetition rate, 1 MHz.

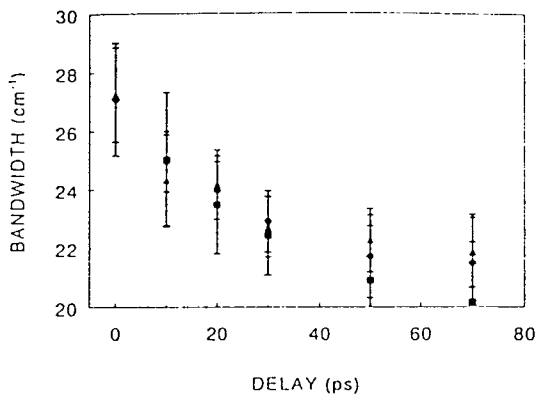

Figure 8. Lorentzian bandwidth of the olefin C=C stretching vibration of S_1 *trans*-stilbene in *n*-hexane vs delay for three pump wavelengths: 303.2 nm (●); 294.4 nm (▲); 285.7 nm (■); probe, 577 nm; repetition rate, 1 MHz.

hexane[56] and 35.96 for acetonitrile.[57] We can understand the changes in the phenyl C=C stretching frequency between the solvents by considering the nature of the optical transition in S_1 tS. Yoshihara et al. describe the S_1 state of tS as a charge-resonance excitation, where the electron density is highly delocalized over the entire molecule.[58] And Waldeck and co-workers have shown that acetonitrile stabilizes the S_1 excitation relative to *n*-hexane, significantly reducing the barrier to isomerization.[8,59] A plausible explanation for these observations is that the more polar solvent would tend to localize a greater fraction of the charge density on the phenyl rings. For this reason, the vibrational motions of the rings are anticipated to be more sensitive to the solvent polarity. An increase in the electron density on the rings will tend to increase the phenyl C=C stretching frequency, as we observe. The increased bandwidth in acetonitrile is also consistent with this picture, since the stronger coupling to the solvent would result in faster dephasing of the vibrational band. We have observed similar effects for the phenyl C=C band in DMSO.[60]

We now consider the peak position and bandwidth changes that occur in the S_1 spectra as a function of delay. As can be seen from Figure 5, there is a substantial change in the C=C region of the S_1 spectrum of tS between 10 and 70 ps. In particular, the olefin band shifts to higher frequencies and the bandwidth narrows. Within experimental error, the peak position and the bandwidth of the phenyl mode remain constant. The same trends are observed in *n*-hexane and acetonitrile, although the magnitudes differ between solvents.

In Figure 7, we plot the peak position of the olefin band in *n*-hexane vs delay for the three pump wavelengths used in this work. There are several important observations from these data. The first is that the peak position shifts to higher frequency with increasing delay for all of the pump wavelengths. In addition, as the amount of excess vibrational energy increases, the peak position at the earliest delays decreases. However, the bandwidth change vs delay for the olefin band is the same for all three pump wavelengths, as shown in Figure 8. We note that the other bands in this spectral region, e.g., 1528 and 1420 cm^{-1}, do not change peak position or bandwidth for any delay at any pump wavelength.

In order to explain these results, we need to account for the following observations. First, the explanation must account for the mode specificity that is observed. Second, it needs to account for the Lorentzian line shape of the vibrational bands. And third, the excitation energy dependence must be accounted for.

The excitation energy dependence of the peak position suggests that some type of vibrational relaxation process must be involved in the interpretation of these results. Previous workers have seen spectroscopic evidence for vibrational relaxation in S_1 tS. Hochstrasser and co-workers observed excitation energy effects in the transient absorption spectra in solution.[61] And Hamaguchi[40] and Kamalov et al.[42] have previously presented evidence for the presence of hot S_1 tS using spontaneous and coherent Raman techniques, respectively, in combination with optical depletion timing. We note that in these examples the authors only observed effects when the excitation frequency was 266 nm.

In order to probe the nature of the vibrational relaxation process, we obtained the anti-Stokes transient Raman spectra of S_1 tS at various delays. (The data are not shown.) As we observed in previous work,[43] the only vibrational band of significant intensity on the anti-Stokes side was the 287-cm^{-1} band, which is a C_6–C–C bending mode. No other bands, particularly bands in the 1500–1600-cm^{-1} region, were observable at any delay times. The ratio of the Stokes and anti-Stokes intensities of the 287-cm^{-1} band was constant at all delays, within experimental uncertainty. The lack of any intensity in the 1500–1600-cm^{-1} region on the anti-Stokes side and the constancy of the ratio of the Stokes to anti-Stokes intensity of the 287-cm^{-1} band strongly suggest that any excess thermal energy in S_1 tS either is dissipated or is in low-frequency vibrational modes that are unobservable under our present experimental conditions. Thus, it is unlikely that the changes in peak position and bandwidth of the olefin C=C stretch are the result of direct intermolecular vibrational relaxation between a hot olefin mode and the solvent. A direct coupling of the vibrational modes to the solvent would also make the mode-specific effects difficult to explain; if the olefin mode were hot, the phenyl mode would likely be hot, as well. We note that several investigators have observed strong anti-Stokes intensity in all vibrational modes for molecules that return to the ground-state potential surface very rapidly.[34,36-38,62] These molecules must dissipate a large amount of vibrational energy (ca., 10000 cm^{-1}) in the process of returning to the ground state. In tS, the amount of excess vibrational energy is significantly smaller since the molecule remains in the excited state.

An alternative explanation involving vibrational relaxation is that of resonance energy exchange via a low-frequency vibration, as has been discussed by Harris and co-workers.[63,64] In their model, a "doorway" state, the olefin C=C stretch in this case, couples anharmonically to an "exchange" mode, a low-frequency vibration in the molecule, perhaps a torsional motion in S_1 tS. The exchange mode exchanges energy with the solvent via resonance energy transfer. The theory predicts that the doorway mode will change both position and bandwidth as the energy is exchanged to the solvent via the low-frequency vibration. Such a model can account for the mode specificity because it is possible for specific doorway modes to couple to the low-frequency exchange modes. Depending on the type of coupling that occurs, it is possible for the doorway mode to either increase or decrease in frequency as the molecule cools.[62] For our data, it is not possible to determine unequivocally the effective temperature of the system because we do not know the frequency of the exchange mode, and the signal-to-noise ratio for the mode-specific dynamics is not high enough. However, the qualitative features of the exchange theory are in good agreement with the experimental observables. The only experimental feature that is not consistent with the exchange theory is that the change in bandwidth is constant as the excitation

frequency is varied. The change in bandwidth should vary with the amount of excess vibrational energy, as we observe with the peak position. This suggests that there may be additional factors that affect the dephasing of the vibrational motion and give rise to the changes in the bandwidth. One possibility is that the bandwidth variation arises from conformational changes associated with the isomerization process.[65]

Other workers have suggested that the S_1 potential energy surface is not one-dimensional but rather is multidimensional.[27,29-31,66] The torsional motion about the olefin–phenyl single bond provides the additional coordinate, as modeled theoretically.[27,31] It is known that the phenyl rings are ~30° out of the plane of the olefin, on the average, in solution.[48,67,68] We assume that in solution there is a distribution of conformations about the torsion coordinate in the ground state. When that distribution is photoexcited to S_1, the degree to which the olefin can delocalize its electron density will depend on the overlap between the phenyl and olefin portions of the molecule. The more planar the phenyl rings, the easier it is for the olefin to remove charge density from the central bond. Thus, the more planar molecules will result in olefin C=C stretching frequencies that are more single bond in character (i.e., at lower wavenumber shifts), and this distribution in conformations would result in a broad line width. Those molecules where the phenyl rings are less planar will give correspondingly higher olefin C=C stretching frequencies. Owing to the more single-bond character of the olefin, the planar molecules would have a slightly higher rate for isomerization. At early times, the population of the more planar molecules would decrease more rapidly than that of the more nonplanar molecules. With time, the apparent frequency of the olefin C=C stretch will shift to higher energy, while the bandwidth would decrease due to an increasing homogeneity of the remaining molecules. These are the trends that we observe in our data. The effects would be mode-specific, as ours are, and the peak position would shift to higher energy, while the bandwidth would narrow as the distribution changes. However, this interpretation suffers from the fact that the lifetimes of S_1 tS are single-exponential in these solvents and the band shapes of the Raman bands are Lorentzian, not Gaussian, suggesting that the observed trends are not due to a distribution of conformations. In an attempt to clarify this issue, we are currently investigating the S_1 Raman spectra of several methyl-substituted stilbenes where multidimensional effects manifest themselves in multiple-exponential fluorescence decay times.[64]

5. Conclusions

We have presented the results demonstrating that picosecond transient Raman spectroscopy can provide microscopic information about the coupling of energy between a photochemical reactant and its solvent environment. In the case of S_1 tS, we observe mode-specific, solvent-dependent variations in several vibrational motions. We observe that the peak position and bandwidth of the phenyl C=C stretch are sensitive to the solvent polarity. The peak position and bandwidth of the olefin C=C stretch change with delay; the degree of the change is dependent on the excitation frequency. We attribute these variations, in part, to vibrational relaxation that occurs via resonance energy exchange involving low-frequency vibrations. While the existing data are difficult to reconcile with a multidimensional potential energy surface for S_1 tS, it is possible that other conformational effects are contributing to the change in bandwidth. More work remains to be done to clarify this issue. We note that we have observed the same types of effects (i.e., mode-specific, solvent-dependent dynamics) in the S_1 Raman spectra of several substituted stilbenes and cyanine dyes.[69] This work demonstrates that the structural specificity of picosecond vibrational spectroscopy provides a powerful approach to the study of the microscopic details in solvent/solute interactions.

Note Added in Revision. Recently, Iwata and Hamaguchi[70] have obtained the transient Raman spectra of S_1 tS in *n*-heptane at one excitation wavelength using a transform-limited picosecond Raman apparatus. With higher time resolution, they observe the same types of spectral changes as we report here. In addition, they observe a distinct difference in the dynamics of the peak position and bandwidth at very early times. They attribute their results both to intramolecular effects and to structural relaxation involving the motion of the surrounding solvent. Their interpretation is consistent with the interpretation we present here.

Acknowledgment. L.A.H. gratefully acknowledges the NSF for support in the form of a graduate fellowship. We acknowledge Coherent, Inc., for the loan of some of the equipment used in these experiments. We also acknowledge The Ohio State University for partial support of this work through the Seed Grant Program. We thank H. Hamaguchi for many fruitful discussions and for communicating results prior to publication.

References and Notes

(1) Fleming, G. R. *Chemical Applications of Ultrafast Spectroscopy*; Oxford University Press: New York, 1986.
(2) Maroncelli, M.; MacInnis, J.; Fleming, G. R. *Science* **1989**, *243*, 1674.
(3) Simon, J. D. *Acc. Chem. Res.* **1988**, *21*, 128.
(4) Barbara, P. F.; Jarzeba, W. *Adv. Photochem.* **1990**, *15*, 1.
(5) Hynes, J. T. In *Theory of Chemical Reaction Dynamics*; Baer, M., Ed.; CRC Press: Boca Raton, FL, 1985.
(6) Bagchi, B. *Annu. Rev. Phys. Chem.* **1989**, *40*, 115.
(7) Zeglinski, D. M.; Waldeck, D. H. *J. Phys. Chem.* **1988**, *92*, 692.
(8) Park, N. S.; Waldeck, D. H. *J. Phys. Chem.* **1990**, *94*, 662.
(9) Velsko, S. P.; Waldeck, D. H.; Fleming, G. R. *J. Chem. Phys.* **1983**, *78*, 249.
(10) Bowman, R. M.; Eisenthal, K. B. *Chem. Phys. Lett.* **1989**, *155*, 99.
(11) Kim, S. K.; Fleming, G. R. *J. Phys. Chem.* **1988**, *92*, 2168.
(12) (a) Lee, M.; Bain, A. J.; McCarthy, P. J.; Han, C. H.; Haseltine, J. N.; Smith, A. B., III; Hochstrasser, R. M. *J. Chem. Phys.* **1986**, *85*, 4341. (b) Lee, M.; Haseltine, J. N.; Smith, A. B., III; Hochstrasser, R. M. *J. Am. Chem. Soc.* **1989**, *111*, 5044.
(13) (a) Courtney, S. H.; Fleming, G. R. *Chem. Phys. Lett.* **1984**, *103*, 443. (b) Courtney, S. H.; Fleming, G. H. *J. Chem. Phys.* **1985**, *83*, 215.
(14) Saltiel, J.; Sun, Y. P. *J. Phys. Chem.* **1989**, *93*, 6246.
(15) Sun, Y. P.; Saltiel, J. *J. Phys. Chem.* **1989**, *93*, 8310.
(16) (a) Troe, J. *J. Phys. Chem.* **1986**, *90*, 357. (b) Schroeder, J.; Troe, J. *Annu. Rev. Phys. Chem.* **1987**, *38*, 163.
(17) Nordholm, S. *Chem. Phys.* **1989**, *137*, 109.
(18) For reviews see: (a) Waldeck, D. H. *Chem. Rev.* **1991**, *91*, 415. (b) Saltiel, J.; Sun, Y. P. In *Photochromism-Molecules and Systems*; Dürr, H., Bouas-Laurent, H., Eds.; Elsevier: Amsterdam, 1990. (c) Hochstrasser, R. *Pure Appl. Chem.* **1980**, *52*, 2683.
(19) Saltiel, J. *J. Am. Chem. Soc.* **1967**, *89*, 1036.
(20) Kramers, H. *Physica* **1940**, *7*, 284.
(21) Rothenberger, G.; Negus, D.; Hochstrasser, R. M. *J. Chem. Phys.* **1983**, *79*, 5360.
(22) Grote, R. F.; Hynes, J. T. *J. Chem. Phys.* **1980**, *73*, 2715; **1982**, *77*, 3736.
(23) Carmeli, B.; Nitzan, A. *J. Chem. Phys.* **1983**, *79*, 393.
(24) Okuyama, S.; Oxtoby, D. W. *J. Chem. Phys.* **1986**, *84*, 5830.
(25) Pollack, E. *J. Chem. Phys.* **1987**, *86*, 3944.
(26) Berne, B. J.; Borkovec, M.; Straub, J. E. *J. Phys. Chem.* **1988**, *92*, 3711.
(27) (a) Agmon, N.; Hopfield, J. J. *J. Chem. Phys.* **1983**, *78*, 6947. (b) Agmon, N.; Hopfield, J. J. *J. Chem. Phys.* **1983**, *79*, 2042. (c) Agmon, N.; Kosloff, K. *J. Phys. Chem.* **1987**, *91*, 1988. (d) Agmon, N.; Rabinovich, S. *Ber. Bunsenges. Phys. Chem.* **1991**, *95*, 278. (e) Rabinovich, S.; Agmon, N. *Chem. Phys. Lett.* **1991**, *182*, 336.
(28) Carmeli, B.; Nitzan, A. *Chem. Phys. Lett.* **1984**, *106*, 329.
(29) Schroeder, J.; Schwarzer, D.; Troe, J.; Voss, F. *J. Chem. Phys.* **1990**, *93*, 2393.
(30) Bagchi, B.; Fleming, G. R. *J. Phys. Chem.* **1990**, *94*, 9.
(31) (a) Berezhkovskii, A. M.; Berezhkovskii, L. B.; Zitserman, V. Yu. *Chem. Phys.* **1989**, *130*, 55. (b) Berezhkovskii, A. M.; Zitserman, V. Yu. *Chem. Phys. Lett.* **1990**, *172*, 235. (c) Berezhkovskii, A. M.; Zitserman, V. Yu. *Physica* **1990**, *A166*, 585.
(32) (a) MacPhail, R. A.; Variyar, J. E. *Chem. Phys. Lett.* **1989**, *161*, 239. (b) MacPhail, R. A.; Monroe, F. C. *Chem. Phys.* **1991**, *152*, 93. (c) Cates, D. A.; MacPhail, R. A. *J. Phys. Chem.* **1991**, *95*, 2209.
(33) Ci, X.; Pereira, M. A.; Myers, A. B. *J. Chem. Phys.* **1990**, *92*, 4708.
(34) (a) Reid, P. J.; Doig, S. J.; Mathies, R. A. *Chem. Phys. Lett.* **1989**, *156*, 163. (b) Reid, P. J.; Doig, S. J.; Mathies, R. A. *J. Phys. Chem.* **1990**, *94*, 8396.
(35) (a) Moore, J. N.; Hansen, P. A.; Hochstrasser, R. M. *J. Am. Chem. Soc.* **1989**, *111*, 4563. (b) Anfinrud, P. A.; Han, C. H.; Lian, T.; Hochstrasser, R. M. *J. Phys. Chem.* **1991**, *95*, 574.
(36) (a) Xu, X. B.; Lingle, R.; Yu, S. C.; Chang, Y. J.; Hopkins, J. B. *J. Chem. Phys.* **1990**, *92*, 2106. (b) Yu, S. C.; Xu, X. B.; Lingle, R.; Hopkins, J. B. *J. Am. Chem. Soc.* **1990**, *112*, 3668. (c) Lingle, R.; Xu, X. B.; Yu, S. C.; Chang, Y. J.; Hopkins, J. B. *J. Chem. Phys.* **1990**, *92*, 4628. (d) Lingle, R.; Xu, X. B.; Yu, S. C.; Zhu, H. P.; Hopkins, J. B. *J. Chem. Phys.* **1990**, *93*, 5667.
(37) (a) Brack, T. L.; Atkinson, G. H. *J. Mol. Struct.* **1989**, *214*, 289. (b) Brack, T. L.; Atkinson, G. H. *J. Phys. Chem.* **1991**, *95*, 2351.

(38) (a) Noguchi, T.; Hayashi, H.; Tasumi, M.; Atkinson, G. H. *Chem. Phys. Lett.* **1990**, *175*, 163. (b) Noguchi, T.; Hayashi, H.; Tasumi, M.; Atkinson, G. H. *J. Phys. Chem.* **1991**, *95*, 3167. (c) Hayashi, H.; Brack, T. L.; Noguchi, T.; Tasumi, M.; Atkinson, G. H. *J. Phys. Chem.* **1991**, *95*, 6797.
(39) (a) Hamaguchi, H.; Kato, C.; Tasumi, M. *Chem. Phys. Lett.* **1983**, *100*, 3. (b) Hamaguchi, H.; Urano, T.; Tasumi, M. *Chem. Phys. Lett.* **1984**, *106*, 153.
(40) (a) Hamaguchi, H. *Chem. Phys. Lett.* **1986**, *126*, 185. (b) Hamaguchi, H. *J. Chem. Phys.* **1988**, *89*, 2587.
(41) Payne, S. A.; Hochstrasser, R. M. *J. Phys. Chem.* **1986**, *90*, 2068.
(42) Kamalov, V. F.; Koroteev, N. I.; Shkurinov, A. P.; Tolcutaev, B. N. *Chem. Phys. Lett.* **1988**, *147*, 335; *J. Mol. Struct.* **1990**, *217*, 19.
(43) Gustafson, T. L.; Roberts, D. M.; Chernoff, D. A. *J. Chem. Phys.* **1983**, *79*, 1559; **1984**, *81*, 3438.
(44) Gustafson, T. L.; Chernoff, D. A.; Palmer, J. F.; Roberts, D. M. In *Time Resolved Vibrational Spectroscopy*; Atkinson, G. H., Ed.; Gordon and Breach: New York, 1987.
(45) Iwata, K.; Weaver, W. L.; Huston, L. A.; Gustafson, T. L. In *Proc. XIIth International Conference on Raman Spectroscopy*; Durig, J. R., Ed.; John Wiley & Sons: London, 1990.
(46) Gustafson, T. L.; Iwata, K.; Weaver, W. L.; Benson, R. L.; Huston, L. A. In *Laser Applications in Life Sciences, Part Two: Lasers in Biophysics and Biomedicine*; Akhmanov, S. A., Poroshina, M. Y., Koroteev, N. I., Toleutaev, B. N., Eds.; Proc. SPIE 1403; SPIE: Bellingham, WA, 1991; p 545.
(47) Warshel, A. *J. Chem. Phys.* **1975**, *62*, 214.
(48) Meič, A.; Güsten, H. *Spectrochim. Acta* **1978**, *27A*, 101.
(49) Palmö, K. *Spectrochim. Acta A* **1988**, *44*, 341.
(50) Baronovic, G.; Meič, Z.; Güsten, H.; Minck, J.; Keresztury, G. *J. Phys. Chem.* **1990**, *94*, 2833.
(51) Tasumi, M.; Urano, T.; Hamaguchi, H. In *Time Resolved Vibrational Spectroscopy*; Atkinson, G. H., Ed.; Gordon and Breach: New York, 1987.
(52) Negri, F.; Orlandi, G.; Zerbetto, F. *J. Phys. Chem.* **1989**, *93*, 5124.
(53) Urano, T.; Hamaguchi, H.; Tasumi, M.; Yamanouchi, K.; Tsuchiya, S.; Gustafson, T. L. *J. Chem. Phys.* **1989**, *91*, 3884.
(54) Weaver, W. L.; Iwata, K.; Gustafson, T. L. Unpublished results.
(55) Iwata, K.; Huston, L. A.; Weaver, W. L.; Gustafson, T. L. Unpublished results.
(56) Riddick, J. A.; Bunger, W. B.; Sakano, T. K. *Organic Solvents*, 4th ed.; John Wiley & Sons: New York, 1986.
(57) Barthel, J.; Bachhuber, K.; Buchner, R.; Gill, J. B.; Kleebauer, M. *Chem. Phys. Lett.* **1990**, *167*, 62.
(58) Yoshihara, K.; Nmiki, A.; Sumitani, M.; Nakashima, N. *J. Chem. Phys.* **1979**, *71*, 2892.
(59) Shivakumar, N.; Hoburg, E. A.; Waldeck, D. H. *J. Chem. Phys.* **1989**, *90*, 2305.
(60) Weaver, W. L.; Huston, L. A.; Iwata, K.; Gustafson, T. L. Unpublished results.
(61) Doany, F. E.; Greene, B. I.; Hochstrasser, R. M. *Chem. Phys. Lett.* **1980**, *75*, 206.
(62) Trulson, M. O.; Dollinger, G. D.; Mathies, R. A. *J. Am. Chem. Soc.* **1987**, *109*, 586; *J. Chem. Phys.* **1989**, *90*, 4274.
(63) Shelby, R. M.; Harris, C. B.; Cornelius, P. A. *J. Chem. Phys.* **1979**, *70*, 34.
(64) Marks, S.; Cornelius, P. A.; Harris, C. B. *J. Chem. Phys.* **1980**, *73*, 3069.
(65) Hamaguchi, H. Personal communication.
(66) Park, N. S.; Waldeck, D. H. *J. Chem. Phys.* **1989**, *91*, 943; *Chem. Phys. Lett.* **1990**, *168*, 379.
(67) Tractteberg, M.; Fransten, E. B.; Mijlhoff, F. C.; Hockstra, A. *J. Mol. Struct.* **1975**, *26*, 57.
(68) Knauss, D. C.; Evans, G. T. *J. Chem. Phys.* **1981**, *74*, 4627.
(69) Huston, L. A.; Iwata, K.; Gustafson, T. L. Unpublished results.
(70) Iwata, K.; Hamaguchi, H. Unpublished results.